

# Chirality Recognition in Menthol and Neomenthol: Preference for Homoconfigurational Aggregation\*\*

Merwe Albrecht, Jan Will, and Martin A. Suhm\*

(–)-L-Menthol is an important flavoring agent, displaying a strong minty odor as well as a pronounced cooling sensation.<sup>[1]</sup> A major source for (–)-L-menthol is peppermint oil, which contains (+)-D-neomenthol as an impurity. These monoterpene alcohols (C<sub>10</sub>H<sub>20</sub>O) represent two out of eight stereoisomeric 5-methyl-2-(1-methylethyl)-cyclohexan-1-ols that result from permutations at the three stereogenic centers in the cyclohexane ring.

A comparison of the eight menthol isomers shows that (–)-menthol (1*R*,2*S*,5*R*) has the strongest cooling property and freshness. (+)-Menthol and (+)-neomenthol are less minty and more musty.<sup>[2]</sup> The relationship between structure and olfaction was analyzed in terms of receptor interaction.<sup>[3]</sup> Structural requirements include a cyclohexane chair conformation with a larger equatorial alkyl group in the 2-position and a smaller group in the 5-position. Furthermore, an equatorial hydrogen-bond acceptor is needed, preferably in the 1-position, and to the right of a virtual observer “sitting in the chair” with the large alkyl group near his head.<sup>[3]</sup> In addition to its specific odor, menthol elicits a strong cooling sensation when applied to skin or mucous membranes;<sup>[1,4]</sup> this sensation is a result of a rather specific stimulation of the thermosensitive TRPM8 cation channel.<sup>[5,6]</sup>

Menthol has been investigated before by electron diffraction,<sup>[7]</sup> NMR<sup>[8]</sup> and IR spectroscopy,<sup>[7,9]</sup> and quantum chemical calculations.<sup>[7,8]</sup> The electron diffraction results show no significant amount of a second conformer at 363 K.<sup>[7]</sup> The NMR study confirms a dominant carbon skeleton conformer<sup>[8]</sup> in solution. Neither of the two methods is sensitive to the OH group conformation. The only known matrix isolation study<sup>[9]</sup> did not consider data for the OH stretching vibration. Existing quantum chemical calculations<sup>[7,8]</sup> also did not investigate the effect of the torsional isomerism of the OH group.

Molecular recognition in the solid state leads to differences between enantiomerically pure and racemic samples. L-Menthol contains columns of winding hydrogen-bonded chains.<sup>[10]</sup> Small differences in the IR spectra compared to those of racemic menthol, and a complex phase behavior as a function of enantiomeric composition suggest a similar

structure.<sup>[11]</sup> However, enantiopure and racemic menthol have very different solid-state vapor pressures.<sup>[12]</sup> This difference, just as the selective olfactory and cold-receptor response to menthol, indicates strong chirality recognition and calls for a detailed study of the way in which menthol enantiomers and diastereoisomers differ in their interaction with other chiral molecules. As a reference for exact quantum chemical modeling of this selective interaction, low-temperature gas-phase investigations of selected complexes would be appropriate.<sup>[13]</sup>

Herein, we describe the investigation into the enantiomer recognition in menthol and neomenthol by looking for spectral differences between the homo- and heteroconfigurational (homo- and heterochiral) dimers generated using supersonic expansion. This self-recognition<sup>[14]</sup> provides the starting point for a more systematic receptor recognition study. The absence of a suitable UV chromophore in the monoterpenes suggests direct absorption IR spectroscopy. The low vapor pressure requires a heatable nozzle, which we have recently interfaced with an FTIR spectrometer.<sup>[15]</sup>

The experimental setup, which involves a pulsed 10 × 0.5 mm<sup>2</sup> double-slit nozzle, is described in the Supporting Information and elsewhere.<sup>[15,16]</sup> The gas mixture for the supersonic expansion was prepared by flowing helium through a heated sample container filled with either the enantiomerically pure or racemic compound that was finely ground and melted (if solid at room temperature) over dried molecular sieves to maintain a large surface.

The observed FTIR spectra in the OH stretching region of enantiopure and racemic menthol and neomenthol are shown in Figure 1 and summarized in Table 1. For menthol, only one dominant monomer band is observed at  $\tilde{\nu} = 3654 \text{ cm}^{-1}$ , close to the previous thermally broadened gas phase value ( $\tilde{\nu} = 3656 \text{ cm}^{-1}$ ).<sup>[7]</sup> Signals from the less abundant monomer conformations are seen at a lower wavenumber. Two well-separated dimer donor bands, shifted to even lower wavenumber, were observed in the spectrum of enantiopure menthol (Figure 1 a). The lower frequency signal corresponds to the dimer with higher abundance. The third band in the spectrum of the aggregates has a steeper concentration dependence and is likely to be a trimer (Figure 1 e). If one half of the menthol is replaced by its enantiomer (Figure 1 b), the intensities of the homochiral dimer bands are reduced by about twofold, as expected for statistical dimerization. The intensity of the band corresponding to the homochiral trimer is decreased by a larger factor, as expected. A new band, corresponding to the heterochiral dimer, emerged between the two bands of the homochiral dimers. The corresponding acceptor bands in the dimers close to the monomer band are

[\*] Dr. M. Albrecht, J. Will, Prof. Dr. M. A. Suhm  
Institut für Physikalische Chemie, Universität Göttingen  
Tammannstrasse 6, 37077 Göttingen (Germany)  
E-mail: msuhm@gwdg.de

[\*\*] This work was supported by the DFG research training group 782 (www.pcg.de) and the FCI. We thank U. Schmitt, M. Nedić, and C. A. Rice for valuable help and discussions.

Supporting information for this article is available on the WWW under <http://dx.doi.org/10.1002/anie.201001565>.

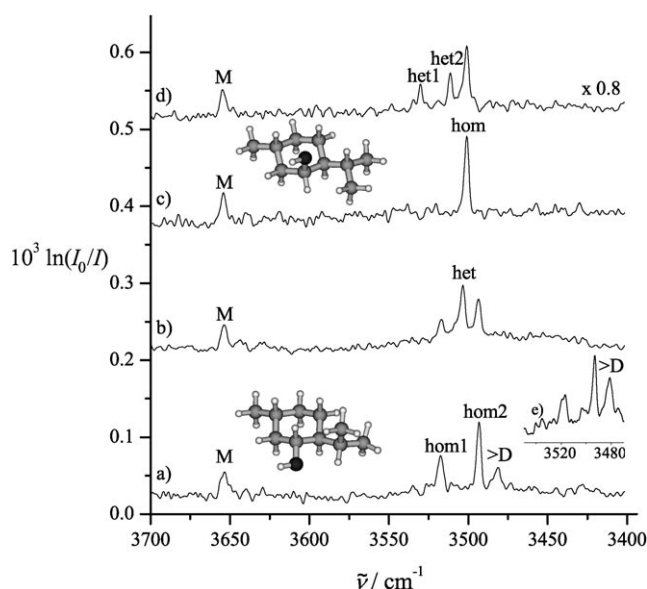


**Figure 1.** Supersonic expansion FTIR spectra of menthol and neomenthol. a) Enantiopure (–)-menthol, b) racemic (±)-menthol, c) enantiopure (+)-neomenthol, d) racemic (±)-neomenthol; monomer bands are marked with M, homochiral and heterochiral dimer bands with hom and het, a larger homochiral cluster with >D. e) shows part of a (–)-menthol spectrum at higher concentration as an insert. The structural inserts represent global minimum structures of menthol (a) and neomenthol (c) with *trans*-OH conformation (C gray, H white, O black). Spectra b–d) are shifted vertically by 0.16, 0.35, and 0.49, respectively.

**Table 1:** Band positions for the O–H stretching vibrations determined in the supersonic expansion FTIR experiment for menthol and neomenthol. Dimer shifts are listed relative to the observed monomer.<sup>[a]</sup>

|                | $\tilde{\nu}(M)$ | $\Delta\tilde{\nu}$<br>(hom1-M) <sup>[b]</sup> | $\Delta\tilde{\nu}$<br>(hom2-M) <sup>[b]</sup> | $\Delta\tilde{\nu}$<br>(het1-M) | $\Delta\tilde{\nu}$<br>(het2-M) |
|----------------|------------------|--|--|---------------------------------|---------------------------------|
| (–)-menthol    | 3654             | –137   | –161   | –                               | –                               |
| (±)-menthol    | 3654             | (–137)   | (–161)   | –150                            | –                               |
| (+)-neomenthol | 3655             | –154   | –  | –                               | –                               |
| (±)-neomenthol | 3655             | (–154)   | –  | –125                            | –144                            |

[a] All values given in  $\text{cm}^{-1}$ . The shift of the higher homochiral cluster  $\tilde{\nu}(>D-M)$  is  $-173 \text{ cm}^{-1}$ .

[b] Homochiral peaks decrease in intensity upon switching to the racemate, values are given in parenthesis.

too weak to be observed because of a lack of hydrogen-bond-induced IR enhancement.

Neomenthol also shows a single band for the OH stretching mode in the monomer (Figure 1c). This band appears at a position similar to that of menthol ( $\tilde{\nu} = 3654.5 \text{ cm}^{-1}$ ), even though the OH group is now in the axial position.<sup>[8]</sup> In the spectrum of the enantiopure neomenthol, a single band representing the OH stretching mode in the dimer is observed (Figure 1c); this band is weaker in the spectrum for racemic neomenthol (Figure 1d). Additionally, two new dimer bands that are blue-shifted compared to that of the homochiral dimer are found. For the C–H stretching region, see Figure S1 in the Supporting Information.

In summary, three bands for the homo- and heterochiral dimers are observed for both menthol and neomenthol. In menthol two of the bands represent homochiral dimers and

one represents a heterochiral dimer. For neomenthol, the opposite situation applies, but in all cases the homochiral dimers show the largest shifts. The observed chirality effects in menthol and neomenthol are much larger than those observed for 2-butanol,<sup>[13]</sup> the prototypical chiral alcohol.<sup>[17]</sup>

The monomer bands lie in a typical range for secondary alcohols (e.g. 2-adamantol), lower than that for a primary alcohol, and higher than that for a tertiary alcohol; this results from the electron-donating effects of the alkyl substituents.<sup>[16]</sup> The red-shifts of the dimer bands span a range of  $\tilde{\nu} = 125$ – $161 \text{ cm}^{-1}$ , exceeding the range found for other secondary alcohols. The smallest shifts are more typical for primary alcohols and indicate competing attractive or repulsive alkyl interactions that weaken the hydrogen bond. The largest shift (hom2) is larger than any shift observed thus far for the OH stretching in alcohol dimers, including nearly all tertiary alcohols.<sup>[16,18]</sup> Such a large shift can be explained by either a good fit between the monomers or an isomerization of the donor OH group in the dimer formation.<sup>[16]</sup> Clearly, the alicyclic substituent serves as a second “functional group” in these alcohols, and modulates the hydrogen-bond interaction.

An accurate quantum chemical prediction of the shifts for the OH stretching modes in menthol dimers will require large basis set frequency calculations at MP2 or CCSD(T) level, which are beyond the current technical capabilities. We have carried out exploratory lower level calculations at the HF/6-21G, B3LYP/6-311 + G\*, B97D/TZVP/TZVPfit, and MP2/6-311 + G\* levels of theory using the Gaussian program.<sup>[19,20]</sup>

Results for menthol monomers, dimers, and trimers and for neomenthol monomers are given in the Supporting Information. HF and B97D calculations were used to search for the most stable dimer structures. However, the ordering of the two most stable monomer conformations on the basis of energy (Table 2) is different from those calculated using the B3LYP and MP2 methods.

For menthol, the most stable conformations are computed to have all substituents in the equatorial positions of the cyclohexane ring.

Similar to previous electron diffraction<sup>[7]</sup> and NMR studies,<sup>[8]</sup> we find that the isopropyl group with approximately a  $60^\circ$  H-C<sub>ipr</sub>-C2-H dihedral angle. Conformations in which the isopropyl group is in another orientation are at least  $4 \text{ kJ mol}^{-1}$  higher in energy (B3LYP, including zero-point energy correction; the four most stable conformers of menthol are shown in Figure S2 in the Supporting Information). The most stable conformer, as determined at the B3LYP and MP2 levels of approximation, has the OH group in a *trans* position with respect to the C2–C1 bond. The energy difference between the most stable conformer and the second most stable conformer *gauche*(–) is small (less than  $2 \text{ kJ mol}^{-1}$ ). Because of the small energy barrier for relaxation, the *gauche* form was nevertheless not observed in the spectra. The enhanced stability of the *trans* conformer may be similar to that of the

**Table 2:** Calculated energy difference ( $\Delta E_0$ ; including harmonic zero-point energy correction) and harmonic wavenumber shift ( $\Delta\omega$ ) of the *gauche*(–)-OH conformation in relation to the *trans*-OH conformation.<sup>[a]</sup>

|            | Method | $\Delta E_0$ [kJ mol <sup>–1</sup> ] | $\Delta\omega$ [cm <sup>–1</sup> ] |
|------------|--------|--------------------------------------|------------------------------------|
| menthol    | HF     | –0.7                                 | –18                                |
|            | B3LYP  | 1.3                                  | –23                                |
|            | MP2    | 1.9                                  | –13                                |
|            | B97D   | –1.8                                 | –22                                |
| neomenthol | HF     | 3.7                                  | +19                                |
|            | B3LYP  | 1.2                                  | +9                                 |
|            | MP2    | 1.5                                  | +12                                |
|            | B97D   | –1.0                                 | +2                                 |

[a] Except for the HF menthol and B97D results, the global minimum conformation is *trans*, which is in agreement with experimental evidence and the robust wavenumber sequence for the most stable conformers.

Gt form of the model compound *n*-propanol:<sup>[21]</sup> a weak hydrogen bond from the  $\gamma$  C–H (in this case from the isopropyl group) to the lone pair of electrons on the oxygen atom can be formed.

Neomenthol differs in the OH group orientation, which is now axial instead of equatorial (Figure 1). This orientation, as given by calculations, places the isopropyl group at a H–C<sub>ipr</sub>–C2–H dihedral angle of about 180°, which is in agreement with the NMR study in solution.<sup>[8]</sup> The most stable OH orientation is again *trans* relative to the C2–C1 bond, and the second most stable is the *gauche*(–) structure.

In agreement with the experimental findings, the OH stretching bands for the *trans* monomer of neomenthol and menthol coincide in the harmonic approximation (e.g.  $\tilde{\nu}$  = 3798 cm<sup>–1</sup> at MP2/6-311 + G\* level). At the B97D level of approximation, the deviation is largest (6 cm<sup>–1</sup>). Calculations in the absence of the *i*Pr group confirm that the OH stretching band for the *trans* conformer is not very sensitive to the position (axial/equatorial) of the OH group. In contrast to menthol, the OH stretching band of the second most stable *gauche*(–) conformer of neomenthol is expected to be blue-shifted (Table 2). Therefore, the *gauche* isomers of both menthol and neomenthol are predicted to be separated by at least  $\tilde{\nu}$  = 25 cm<sup>–1</sup> at all investigated levels of theory. The combined study of the spectra for both menthol and neomenthol monomers clearly supports the assignment of a *trans*-OH group in both cases. Furthermore, it shows that the relative energies predicted at B97D level of approximation are qualitatively wrong. The ability of IR spectroscopy to clearly distinguish between rotational isomers around the C–O bond is confirmed to be superior to using NMR and electron diffraction methods.

Compared to the straightforward modeling of the monomer, a quantum chemical description of the hydrogen-bonded dimers is more challenging. Both stable OH conformations (*trans* and *gauche*(–)) of the monomer have to be considered in the dimer because the low-energy barrier might be overcome for a more stable dimer orientation as seen in smaller alcohol dimers.<sup>[21]</sup> Furthermore, dispersion interactions are expected to play an essential role in determining the preferred structures by rotation around the hydrogen-bond axis, but the hydrogen bond itself is still responsible for a

major fraction of the cohesion energy. The calculations at the B97D level of approximation (see the Supporting Information) indicate that there are more stable homochiral dimers than heterochiral dimers. Their stability and stretching frequency for the donor OH group is strongly influenced by the interplay between hydrogen bonding and London dispersion forces. Although this result is in qualitative agreement with experimental data, dispersion-corrected hybrid density functionals or complete basis set extrapolations at the MP2/CCSD(T) level of approximation would be helpful. The B97D results suffer from the prediction of the wrong monomer sequence and a drastic overestimation of the hydrogen-bond shifts.

The band red-shifted by  $\tilde{\nu}$  = 173 cm<sup>–1</sup> is accounted for by a C<sub>3</sub>-symmetric homochiral trimer (see Figure S8 in the Supporting Information). Its dissociation energy,  $D_0$ , relative to three *trans* monomers is 94 kJ mol<sup>–1</sup> (B97D) and 56 kJ mol<sup>–1</sup> (B3LYP) which is between two and three times the dimer dissociation energy. Steric demands do not impede the formation of ring clusters, in fact a comparison of the B3LYP and B97D structures (see Figure S8 in the Supporting Information) shows an attractive contribution from the dispersion forces. The predicted red-shift (9% larger than the strongest dimer red-shift at B97D level) of the doubly degenerate IR active band relative to the *trans* monomer is in agreement with the experimental value (7%). Therefore, the band at  $\tilde{\nu}$  = 3481 cm<sup>–1</sup> in the spectrum of enantiopure menthol is assigned to a homochiral C<sub>3</sub>-symmetric trimer. The heterochiral trimer was not observed, likely a result of either the greater structural and spectral diversity or a less favorable packing of the configurationally heterogeneous alkyl groups.

The latter also seems to be the case for the bulk crystal, which has a substantially higher vapor pressure in the racemic case than in the enantiopure case, at least at low temperatures.<sup>[12]</sup> We have reinvestigated this finding, and the relative vapor pressures were determined using a quadrupole mass spectrometer, which is described in more detail elsewhere<sup>[22]</sup> and in the Supporting Information. For enantiopure menthol, the measured vapor pressure curve between 273 and 293 K is consistent with a sublimation enthalpy of (95 ± 2) kJ mol<sup>–1</sup>, which is in agreement with a previous study.<sup>[12,23]</sup> The racemic sample has almost twice (1.9 ± 0.2 times) the amount of the enantiopure vapor pressure between 273 and 283 K. A doubling of the vapor pressure would be consistent with conglomerate formation. However, at 293 K the vapor pressure ratio between the racemic and enantiopure forms drops to 1.5 ± 0.2, a value that is closer to the well-studied case of trifluoromethyl lactic acid.<sup>[22]</sup> This result is indicative of a phase change in the racemate, consistent with earlier observations of complex phase diagrams of menthol.<sup>[11]</sup> After a long storage period, a less volatile racemic phase is occasionally observed over an extended temperature range, whereas the vapor pressure of the enantiopure form remains stable. Construction of the sublimation phase diagram<sup>[24]</sup> is nontrivial because of the existence of several polymorphs and mutual solid-phase solubility.<sup>[11]</sup> We plan to study this interesting chirality dependent sublimation behavior through a combination of systematic vapor pressure studies and infrared microscopy. There is a potential for spontaneous low

temperature racemate separation by using enantiopure seed crystals, as proposed in reference [12].

In summary, menthol can be prepared in a single OH monomer conformation and shows a marked chirality discrimination behavior upon self-aggregation. Two homochiral dimers are detected by supersonic expansion FTIR spectroscopy, the more abundant one featuring a record value for the hydrogen-bond-induced red-shift of the OH stretching band for a secondary alcohol dimer. The cyclic homochiral trimer shows a single IR-active band. In contrast, only a single heterochiral dimer and no specific heterochiral trimer were found. This microscopic homochiral binding preference is also reflected in a reduced vapor pressure of the enantiopure crystals, in particular at low temperature. An inversion at the asymmetric carbon center carrying the OH group (neomenthol) helps in assigning the monomer conformations and leads to a rather different molecular recognition pattern. Only a single homochiral dimer is now formed, whereas two more weakly bound heterochiral dimers are observed for the racemic sample. These strong chirality recognition phenomena at the level of self-aggregation are in line with the pronounced chirality recognition and diastereoselectivity of the organoleptic receptor response for menthol.<sup>[2,3]</sup> Therefore, we plan to extend our studies to molecular complexes mimicking possible receptor–substrate interactions. Furthermore, the spectroscopic findings invite high-level quantum chemical modeling. A quantum chemical approach which is able to describe the stability and red-shift trends for the hydrogen-bonded clusters found in this work has better prospects of explaining menthol receptor action from first principles.<sup>[25]</sup>

Received: March 16, 2010

Published online: July 22, 2010

**Keywords:** dimers · FT-IR spectroscopy · menthol · molecular recognition · hydrogen bonding

- [1] R. Eccles, *J. Pharm. Pharmacol.* **1994**, *46*, 618–630.
- [2] R. Emberger, R. Hopp in *Topics in Flavour Research* (Eds.: R. G. Berger, S. Nitz, P. Schreier), H. Eichhorn, Frankfurt, **1985**, pp. 201–218.
- [3] M. Chastrette, E. Rallet, *Flavour Fragrance J.* **1998**, *13*, 5–18.
- [4] T. Patel, Y. Ishiui, G. Yosipovitch, *J. Am. Acad. Dermatol.* **2007**, *57*, 873–878.
- [5] D. D. McKemy, W. M. Neuhausser, D. Julius, *Nature* **2002**, *416*, 52–58.
- [6] S.-E. Jordt, D. D. McKemy, D. Julius, *Curr. Opin. Neurobiol.* **2003**, *13*, 487–492.
- [7] T. Egawa, M. Sakamoto, H. Takeuchi, S. Konaka, *J. Phys. Chem. A* **2003**, *107*, 2757–2762.
- [8] J. Härtner, U. M. Reinscheid, *J. Mol. Struct.* **2008**, *872*, 145–149.
- [9] W. M. Coleman III, B. M. Gordon, B. M. Lawrence, *Appl. Spectrosc.* **1989**, *43*, 298–304.
- [10] P. Bombicz, J. Buschmann, P. Luger, N. X. Dung, C. B. Nam, *Z. Kristallogr.* **1999**, *214*, 420–423.
- [11] M. Kuhnert-Brandstätter, R. Ulmer, *Arch. Pharma.* **1974**, *307*, 497–503, 539–549.
- [12] J. S. Chickos, D. L. Garin, M. Hitt, G. Schilling, *Tetrahedron* **1981**, *37*, 2255–2259.
- [13] A. Zehnacker, M. A. Suhm, *Angew. Chem.* **2008**, *120*, 7076–7100; *Angew. Chem. Int. Ed.* **2008**, *47*, 6970–6992.
- [14] N. Borho, T. Häber, M. A. Suhm, *Phys. Chem. Chem. Phys.* **2001**, *3*, 1945–1948.
- [15] M. Albrecht, C. A. Rice, M. A. Suhm, *J. Phys. Chem. A* **2008**, *112*, 7530–7542.
- [16] C. Cézar, C. A. Rice, M. A. Suhm, *J. Phys. Chem. A* **2006**, *110*, 9839–9848.
- [17] A. K. King, B. J. Howard, *Chem. Phys. Lett.* **2001**, *348*, 343–349.
- [18] T. Häber, U. Schmitt, M. A. Suhm, *Phys. Chem. Chem. Phys.* **1999**, *1*, 5573–5582.
- [19] M. J. Frisch et al. Gaussian03, Revision D.01. Gaussian, Inc., Wallingford CT, **2004**.
- [20] M. J. Frisch et al. Gaussian09, Revision A.02. Gaussian, Inc., Wallingford CT, **2009**.
- [21] T. N. Wassermann, P. Zielke, J. J. Lee, C. Cézar, M. A. Suhm, *J. Phys. Chem. A* **2007**, *111*, 7437–7448.
- [22] M. Albrecht, V. A. Soloshonok, L. Schrader, M. Yasumoto, M. A. Suhm, *J. Fluorine Chem.* **2010**, *131*, 495–504.
- [23] J. S. Chickos, W. E. Acree, Jr., *J. Phys. Chem. Ref. Data* **2002**, *31*, 537–698.
- [24] M. Farina, G. Di Silvestro, *Mol. Cryst. Liq. Cryst.* **1988**, *161*, 177–198.
- [25] M. A. Suhm, *Adv. Chem. Phys.* **2009**, *142*, 1–57.